



## Measurement in a wind tunnel of dry deposition velocities of submicron aerosol with associated turbulence onto rough and smooth urban surfaces

Pierre Roupsard, Muriel Amielh, Didier Maro, Alexis Coppalle, Hubert Branger, Olivier Connan, P. Laguionie, D. Hébert, M. Talbaut

### ► To cite this version:

Pierre Roupsard, Muriel Amielh, Didier Maro, Alexis Coppalle, Hubert Branger, et al.. Measurement in a wind tunnel of dry deposition velocities of submicron aerosol with associated turbulence onto rough and smooth urban surfaces. *Journal of Aerosol Science*, 2013, 55, pp.12-24. 10.1016/j.jaerosci.2012.07.006 . hal-00760178

**HAL Id: hal-00760178**

**<https://hal.science/hal-00760178>**

Submitted on 4 Dec 2012

**HAL** is a multi-disciplinary open access archive for the deposit and dissemination of scientific research documents, whether they are published or not. The documents may come from teaching and research institutions in France or abroad, or from public or private research centers.

L'archive ouverte pluridisciplinaire **HAL**, est destinée au dépôt et à la diffusion de documents scientifiques de niveau recherche, publiés ou non, émanant des établissements d'enseignement et de recherche français ou étrangers, des laboratoires publics ou privés.

Manuscript Number:

Title: MEASUREMENT IN A WIND TUNNEL OF DRY DEPOSITION VELOCITIES OF SUBMICRON AEROSOL WITH ASSOCIATED TURBULENCE ONTO ROUGH AND SMOOTH URBAN SURFACES

Article Type: Regular Paper

Keywords: dry deposition; deposition velocity; submicron aerosol; urban surfaces; wind tunnel

Corresponding Author: Mr. Pierre Roupsard, M.D.

Corresponding Author's Institution: IRSN

First Author: Pierre Roupsard, M.D.

Order of Authors: Pierre Roupsard, M.D.; Muriel Amielh, PhD; Denis Maro, Professor; Alexis Coppalle, Professor; Hubert Branger, PhD; Olivier Connan, PhD; Philippe Laguionie, PhD; Didier Hébert; Martine Talbaut, PhD

Please find as attached files a manuscript untitled:

“Measurement in a wind tunnel of dry deposition velocities of submicron aerosol with associated turbulence onto rough and smooth urban surfaces”,

co-authored by : P. Roupsard, M. Amielh, D. Maro, A. Coppalle, H. Branger, O. Connan, P. Laguionie, D. Hébert and M. Talbaut; for submission to “Journal of Aerosol Science”.

Best regards.

Pierre Roupsard

1 **HIGHLIGHTS:**

- 2 Submicron aerosol deposition on urban surfaces is studied in a wind tunnel.
- 3 Associated turbulent parameters are measured or estimated with a hot wire anemometry.
- 4 Settling has an influence on deposition on smooth surface and at low wind speed.
- 5 Submicron aerosol deposition is dependent on turbulent deposition processes.

**MEASUREMENT IN A WIND TUNNEL OF DRY DEPOSITION VELOCITIES OF SUBMICRON AEROSOL WITH ASSOCIATED TURBULENCE ONTO ROUGH AND SMOOTH URBAN SURFACES**

P. Rounsard<sup>1\*</sup>, M. Amielh<sup>2</sup>, D. Maro<sup>1</sup>, A. Coppalle<sup>3</sup>, H. Branger<sup>2</sup>, O. Connan<sup>1</sup>, P. Laguionie<sup>1</sup>, D. Hébert<sup>1</sup> and M. Talbaut<sup>3</sup>.

<sup>1</sup>Laboratoire de Radioécologie de Cherbourg-Octeville (LRC), Institut de Radioprotection et de Sûreté Nucléaire (IRSN), 50130 Cherbourg-Octeville, France.

pierre.roupsard@irsn.fr; denis.maro@irsn.fr; olivier.connan@irsn.fr; philippe.laguionie@irsn.fr; didier.hebert@irsn.fr

<sup>2</sup>Institut de Recherche sur les Phénomènes Hors Equilibre (IRPHE), CNRS, UMR-7342, 13384 Marseille, France.

amielh@irphe.univ-mrs.fr; branger@irphe.univ-mrs.fr

<sup>3</sup>Complexe de Recherche Interprofessionnel en Aérothermochimie (CORIA), UMR-6614, 76801 Saint-Etienne du Rouvray, France.

alexis.coppalle@coria.fr; martine.talbaut@coria.fr

\*CORRESPONDING AUTHOR: pierre.roupsard@irsn.fr

Tel +33 2 33 01 41 00

Fax +33 2 33 01 41 30

Laboratoire de Radioécologie de Cherbourg-Octeville

Rue Max-Pol Fouchet

50130 Cherbourg-Octeville, France

**ABSTRACT:**

In the event of accidental discharges of radionuclides in particulate form by a nuclear plant, dry deposition is the only transfer pathway under dry atmospheric conditions. In this case, for the urban environment, these deposits must be assessed precisely in the urban canopy to estimate the doses potentially received by the population. The objectives of this wind tunnel study are to measure dry deposition velocities of a submicron fluorescein aerosol onto horizontal and vertical urban surfaces of glass, cement facing and grass for several wind speeds and to measure the turbulence parameters associated with these deposition velocities. These deposition velocities are then compared to data of the literature and to the

results of two models for dry deposition. The dry deposition velocity of the fluorescein aerosol increases with the intensity of the turbulence. This highlights the importance of the turbulent processes of impaction and interception in deposition. However, the ratio of dry deposition velocity to friction velocity depends on the surface type. It depends on the turbulence conditions in the boundary layer. These turbulent dry deposition processes thus vary in importance depending on the studied surface. Finally, settling represents a significant part of the deposition for low wind speeds and for smooth surfaces. This wind tunnel study permits the study of the deposition as a function of turbulent processes. It should be supplemented by *in situ* experiments to take into account all the physical processes involved under real conditions.

**KEYWORDS:** Dry Deposition, Deposition Velocity, Submicron Aerosol, Urban Surfaces, Wind Tunnel.

## 44 I. Introduction

45 In a polluted atmosphere or during transit of a plume containing stable or radioactive pollutants, and in the  
46 absence of rainfall events, dry deposition is the only transfer pathway from the air to the surface for  
47 particles and pollutants. At present, this dry deposition has been studied especially on natural surfaces  
48 representing the first link in the human food chain, but very little in the urban environment (Kelly, 1987;  
49 Fowler *et al.*, 2009). However, a significant portion of the human population is concentrated in the urban  
50 environment, and in the case of passage of a radioactive plume, the quantity of radionuclides deposited  
51 by aerosols must be taken into account in estimating the dose rates received by the population (Kelly,  
52 1987). Precise assessment of the transfer of pollutants by dry deposition of aerosols can thus be very  
53 important, and the lack of significant data for the urban environment is now acknowledged. Dry deposition  
54 of aerosols depends on the aerosol diameter, the deposition surface (the roughness and temperature, for  
55 example) and the turbulence conditions (Sehmel, 1980). Therefore aerosols do not deposit  
56 homogeneously in the urban environment. In the case of radioactive pollutants, this deposition must be  
57 studied for various surfaces, on a wall or street level, and not for an urban canopy, on a neighbourhood or  
58 city level, because the distribution of the deposits must be known precisely to assess the doses received  
59 by the residents. The dry deposition velocity is the coefficient used to quantify the transfer of aerosol  
60 particles by dry deposition in the environment. Most of the measurements of dry deposition velocities on  
61 urban surfaces in urban environments were conducted by Roed (1983, 1985, 1987) as a result of the  
62 fallout from nuclear tests and the Chernobyl accident, and by Pesava *et al.* (1999) and Maro *et al.* (2010)  
63 with a tracer aerosol generated *in situ*. However, these deposition velocities are not associated with  
64 precise measurements of turbulence or local meteorology. Presently, there are very few experimental  
65 data related to turbulent parameters for urban environments and surfaces. As a result there are significant  
66 uncertainties in the use of predictive models of deposition for this environment (Fowler *et al.*, 2009).  
67 Urban environments are complex and heterogeneous from the point of view of the turbulence and  
68 measurements under simple conditions should aid in understanding the deposition processes and  
69 quantifying deposition velocities on urban surfaces. The wind tunnel is an advantageous tool. It can be  
70 used as an initial approach to quantifying dry deposition velocities as a function of a restricted number of  
71 controlled parameters and reproducible experiments can be conducted. Dry deposition has already been  
72 the subject of wind tunnel studies, on natural surfaces (Chamberlain, 1967) or on smooth and rough  
73 substrates (Liu and Agarwal, 1974; Horvath *et al.*, 1996; Toprak *et al.*, 1997; Dai *et al.*, 2001), but rather  
74 for micron particles. However, the accumulation mode of the atmospheric aerosol ( $0.1 \mu\text{m} \leq d_p \leq 1 \mu\text{m}$ ) is

the mode that is the primary vector for chemical pollutants and radionuclides. It is the mode on which the surface distribution of the atmospheric aerosol is centred (Gründel and Porstendörfer, 2004; Van Dingenen *et al.*, 2004; Papastefanou, 2008). Moreover, it transports these pollutants over large distances from a source to the urban environments, due to a relatively long residence time in the atmosphere (Jaenicke, 1988; Papastefanou, 2006). While the deposition of particles greater than a micrometre most often studied is strongly affected by sedimentation, deposition of submicron aerosols, which are less studied, results from the contribution of several physical processes (Brownian diffusion, impaction, interception). The main objective of this study is to quantify dry deposition velocities of a submicron aerosol on horizontal and vertical urban surfaces, for several wind speeds and under isothermal conditions in the wind tunnel. Various turbulent boundary layer conditions are thus encountered. These turbulence conditions associated with the dry deposition velocities are quantified by hot wire anemometer measurements and focus especially on determination of the friction velocities. Finally, the data from this study are compared to data in the literature and to operational models, solved analytically, developed for smooth surfaces (Lai and Nazaroff, 2000) and natural canopies (Zhang *et al.*, 2001).

## II. Experimental setup

### II.1 The wind tunnel and the studied surfaces

The experiments were conducted in a recirculating wind tunnel of the IRPHE (University of Aix-Marseille, campus of Luminy, Marseille, France). The experimental test section is a glass channel with a stainless steel base 8650 mm long and a cross-section 280 mm high and 640 mm width. Airflow speeds between 0.5 and 19 m s<sup>-1</sup> can be generated. Deposition was studied on horizontal conventional glass surfaces, cement facing and synthetic grass in a first experimental campaign (Fig. 1.a), then on vertical conventional glass and cement facing surfaces in a second campaign (Fig. 1.b). The commercial names of the materials and the roughness parameters of the cement facing (Flori *et al.*, 2007) and synthetic grass are listed in Table 1. The roughness parameters of the cement facing measured by laser roughness measurements are the arithmetic mean deviation of the profile  $R_a$ , the standard deviation of the profile  $R_q$ , the valley depth of the profile  $R_v$  and the peak height of the profile  $R_p$ . The synthetic grass is composed of primary straight blades grouped into tufts, and thinner and shorter curly blades included in the canopy to make it denser. The parameters characterising the synthetic grass were determined by the authors for the primary straight blades and are the average canopy height  $h_c$ , the length of the straight blades  $l_b$ , the width of these blades  $w_b$ , the number of tufts per square metre  $n_t$  and the number of straight blades per



square metre  $n_b$ . During the experiments on horizontal surfaces, the bottom of the test section was successively completely covered by each type of surface to develop the boundary layers and turbulence conditions characteristic of each surface.

Table 1: characteristics of the studied surfaces.

	Conventional glass	Cement facing	Synthetic grass
<b>Commercial name</b>	Planilux®, Saint-Gobain	Fema®-Therm-Mineralputz 5 mm	"Romana"
<b>Roughness parameters</b>	Glass thickness = 4 mm	$R_a = 0.57 \text{ mm}$	$h_c = 34 \pm 2 \text{ mm}$
		$R_q = 0.74 \text{ mm}$	$l_b = 38.4 \pm 1.9 \text{ mm}$
		$R_v = 2.36 \text{ mm}$	$w_b = 1.2 \pm 0.1 \text{ mm}$
		$R_p = 1.86 \text{ mm}$	$n_t = 10364 \text{ m}^{-2}$
			$n_b = 164675 \text{ m}^{-2}$

In the same way, a vertical wall of the test section was successively covered with conventional glass and cement facing, to measure deposition on a vertical wall. It should be noted that glass cover the walls in the form of a pavement of square plates 200 mm on a side, while the cement facing and synthetic grass covered the wind tunnel homogeneously and continuously. To study deposition over a broad range of wind speeds that can be encountered in the urban environments, airflows of speeds  $u_{ref}$  of 1.3, 5.0 and  $9.9 \text{ m s}^{-1}$  were generated in the test section. The turbulence was quantified above all the horizontal surfaces.

## II.2 Quantification of the dry deposition velocity $V_d$

The dry deposition velocity  $V_d$  ( $\text{m s}^{-1}$ ) of an aerosol is defined by Chamberlain and Chadwick (1953, in Sehmel, 1980) as the ratio of the surface flux of dry deposition  $F$  ( $\text{kg m}^{-2} \text{ s}^{-1}$ ; by convention a deposition flux is negative) by the average concentration of the aerosol in the air  $C$  ( $\text{kg m}^{-3}$ ) at a given height (1).

$$V_d = \frac{-F}{C} \quad (1)$$

A common approach to measure dry deposition velocities is to use a stable or radioactive chemical tracer for the studied aerosol. This method has the advantage of directly measuring a quantity of tracer, and thus of particles, in number or in mass. The deposition flux  $F$  is calculated according to (2),  $M_{\text{substrate}}$  (kg) is the mass of tracer,  $A_{\text{substrate}}$  ( $\text{m}^2$ ) is the total surface of the substrate sample, and  $t$  (s) is the duration of the experiment.

$$-F = \frac{M_{\text{substrate}}}{A_{\text{substrate}} t} \quad (2)$$

The average concentration  $C$  is calculated according to (3), with  $M_{\text{filter}}$  (kg) the mass of tracer collected on the filter with an airflow rate  $Q_{\text{filter}}$  ( $\text{m}^3 \text{s}^{-1}$ ) over the same duration  $t$ .

$$C = \frac{M_{\text{filter}}}{Q_{\text{filter}} t} \quad (3)$$

A slightly polydispersed monomodal submicron dry fluorescein aerosol (uranine,  $\rho = 1500 \text{ kg m}^{-3}$ ) generated with a pneumatic generator is used as a tracer. The operating principle of this generator is described in French standard NF X 44-011. A fluorescein solution is nebulised, the produced droplets are sorted by centripetal filters, then entrained and dried by a dry air flow to obtain a dry solid fluorescein aerosol. The granulometric mass distribution of this aerosol was measured by three samplings with a Dekati (LPI) low pressure cascade impactor (separation of the particles over 12 stages of cutoff diameters between 24 nm and 9.55  $\mu\text{m}$ ) and gave on average an aerodynamic mass median diameter  $d_{\text{amm}}$  of  $0.27 \pm 0.07 \mu\text{m}$  with a geometric standard deviation of  $2.06 \pm 0.23$  (Fig. 2). The air recirculation in the wind tunnel allows to generate particles only for the first two minutes of the experiment and to let the concentration to decrease with time until the end of the experiment. Substrate samples are removed at the end of the fifteen minutes of the experiment. The generated aerosol is introduced at the outlet of the test section to be mixed with air in the recirculation section of the wind tunnel so that its concentration will be homogeneous over the test section inlet. It is injected at the centre of the cross-section with a horizontal copper injection nozzle regularly pierced along a line oriented toward the outlet duct with an airflow rate of  $10.8 \text{ m}^3 \text{h}^{-1}$ . Finally, the air in the test section is renewed between experiments by extracting air towards the exterior. The dry deposition fluxes are measured by exposure of samples (square plates 200 mm on a side composed of the studied substrates) to the fluorescein aerosols for a the experiment time. Samples are used for several experiments. After they are rinsed with distilled water and dried at room temperature, the substrates are placed in the test section with great care so as not to pollute them with fluorescein deposited on the walls of the test section. The static electrical charge is consistently removed from the synthetic grass samples by spraying the blades with denatured ethanol. The charge state of these specimens is then checked with a fieldmeter (Eltex EMF 58). During the experiments on horizontal substrates, three rows of three samples placed across the width of the test section are incorporated into the substrate studied at various distances from the test section inlet. These distances from the inlet are also called “fetch” (m). The edges of these specimens adjoin the substrate surfaces covering the base of the test section. The leading edges of each row of samples are located at

1.0, 5.0 and 6.8 m from the inlet. Each type of substrate is studied separately, as the base of the section is completely covered by a single type of substrate. To measure dry deposition velocities on vertical surfaces, the vertical wall used is covered in the same way with the studied substrate, from the test section inlet to 6 m inside the test section. Three samples are intercalated lengthwise into this vertical wall, with leading edges at 4.8, 5.0 and 5.2 m, to measure the dry deposition fluxes. These specimens are centred in height, 40 mm from the base of the test section. In parallel, samples are taken on cellulose filters (Whatman 1440-047) throughout the exposure time of the specimens to the aerosol in order to quantify its concentration in the air of the test section. Bent copper sampling tubes with a 10 mm inside diameter are introduced from the top of the section so as not to perturb the flow above the studied surfaces and connected to filter holders with 500 mm long fluoroelastomer tubing. During the experiments on horizontal substrates, three samples are taken on filters 10 mm above the surface halfway across the test section, downstream of the specimens, with the inlet of the tube just behind each row of samples (fetch = 1.2, 5.2 and 7.0 m) so as not to perturb the flow over the specimens and thus not to perturb deposition. Likewise, for the experiments on vertical substrates, a sample is taken on a filter just behind the third specimen, 10 mm from the wall, halfway up the test section. In each experiment, a sample is taken on a filter at the centre of the test section, 5.2 m from its entrance, to control *a posteriori* the homogeneity of the particle concentration in the air in the section during the experiment. Collection flow rates are between 7.6 and 8.6 L min<sup>-1</sup> and are checked with a TSI 4000 Series mass flowmeter. The samples and filters are carefully removed, wrapped in aluminium foil to avoid any pollution, and then treated for measurement. Fluorescein is hydrophilic, thus the deposited particles are dissolved simply by rinsing the surface with a pH 9 solution of ammonia water using a syringe (with successive rinsings with the same solution for the glass and cement facing) or directly by soaking (synthetic grass). The filters are immersed directly in the ammonia water to dissolve the filtered fluorescein particles. These solutions are measured with a fluorescence spectrometer (Jobin Yvon Horiba FluoroMax-3) to determine  $M_{\text{substrate}}$  and  $M_{\text{filter}}$ . The background fluorescence of each type of surface is subtracted from the measurement result. Experiments are conducted at least twice to ensure their repeatability.

### II.3 Estimation of the turbulent parameters

In the wind tunnel, in the absence of heat exchange on the studied surface, the turbulent parameter mainly associated with  $V_d$  is the friction velocity  $u_*$  (m s<sup>-1</sup>) because it quantifies mechanical turbulence that enhances the aerosol deposition. Also, it is one of the parameters necessary in modelling  $V_d$  in confined environments (Lai and Nazaroff, 2000) or *in situ* (Zhang *et al.*, 2001). It quantifies the turbulence

generated by shear of a flow over a surface and is used as a reference velocity near the wall. The friction velocity is estimated with (4) by measuring  $\tau_p$  ( $\text{kg m}^{-1} \text{s}^{-2}$ ), the frictional or shear stress at the wall, with  $\rho$  ( $\text{kg m}^{-3}$ ) the fluid density.

$$u_* = \sqrt{\frac{\tau_p}{\rho}} \quad (4)$$

It can also be estimated with (5) using velocity profile measurements above the surface.

$$\frac{u(z)}{u_*} = \frac{1}{\kappa} \ln \frac{z-d}{z_0} \quad (5)$$

$$\frac{u(z)}{u_*} = \frac{1}{\kappa} \ln \frac{z-d}{k_s} + B \quad (6)$$

In (5),  $u(z)$  ( $\text{m s}^{-1}$ ) is the mean velocity in the flow direction measured at the vertical position  $z$  (m), and  $\kappa$  (0.4),  $d$  (m) and  $z_0$  (m) are respectively the Von Karman constant, the displacement height and the aerodynamic roughness height. The friction velocity can be estimated by fitting this relation in the logarithmic overlap area of the velocity profile of a developed turbulent boundary layer;  $u_*$ ,  $d$  and  $z_0$  are then the parameters to be fitted. The aerodynamic roughness height is flow-dependent for dynamically smooth flows and depends on roughness geometry for fully rough flows (Raupach *et al.*, 1991). For synthetic grass,  $z_0$  is equal to  $0.13h_c$  (Tanner and Pelton, 1960, Stanhill, 1969 in Raupach *et al.*, 1991). For cement facing,  $z_0$  is determined from (5) and (6), and equal to  $k_s \exp(-B\kappa)$  ( $B = 8.5$ ; Schlichting, 1968), with  $k_s = R_v + R_p$ . For glass,  $d$  is equal to zero and  $z_0$  can vary. The relative turbulence intensity  $I$  (%) is another dimensionless magnitude that quantifies the turbulent agitation ( $u'$ ,  $w'$ ) of a flow by comparison to the average motion ( $\bar{u}$ ) at a distance  $z$  from the wall. The relative turbulence intensities for the components  $u$  and  $w$  ( $I_u$  and  $I_w$ ) can be calculated according to (7.a) and (7.b).

$$I_u = \frac{\sqrt{\overline{u'^2}}}{\bar{u}}; \quad I_w = \frac{\sqrt{\overline{w'^2}}}{\bar{u}} \quad (7.a); (7.b)$$

With this magnitude, turbulence can be classified into three categories: low (1%), medium (10%) and high (20% and more). The turbulent parameters were estimated in absence of aerosol injection for horizontal surfaces using hot-wire anemometry operating at high frequency. The system used is a probe with two crossed hot wires (type 55P61) combined with a *Streamline* anemometry system (Dantec Dynamics). It measures  $u$ , the horizontal component of velocity in the flow direction, and  $w$ , the vertical component, at high frequencies (2.5 kHz for  $u_{\text{ref}} = 1.3 \text{ m s}^{-1}$  and 10 kHz for  $u_{\text{ref}} = 5.0$  and  $9.9 \text{ m s}^{-1}$ ,  $u_{\text{ref}}$  measured at the center of the test section of the wind tunnel) with a 50 seconds acquisition duration in each position.

208 These turbulence measurements were conducted above each surface type for each  $u_{ref}$  and for each  
 209 fetch above the centre of the central substrate sample, by vertical profiles of 40 points between  
 210  $z = 2.5$  mm and  $z = 200$  mm above the roughnesses of the surfaces.

### 211 III. Results and discussions

#### 212 III.1 Dry deposition velocities $V_d$

213 The measured concentrations of aerosols in the air show no significant difference between the sample in  
 214 the centre of the test section and samples 10 mm from the walls during the experiments (median  
 215 deviation of 6.6%) and show homogenisation of the aerosol concentration in the air recirculation circuit of  
 216 the wind tunnel. The average dry deposition velocities on each type of horizontal surface are calculated  
 217 from the deposition fluxes at 1.0, 5.0 and 6.8 m from the test section inlet and the associated  
 218 concentrations for each flow speed. They show neither variation with the fetch, nor a notable difference  
 219 between the specimens at the centre of the row and those on the sides. The average dry deposition  
 220 velocities calculated for each type of surface, horizontal and vertical, and for each airflow speed  $u_{ref}$  are  
 221 shown in Table 2 and Fig. 3. The dry deposition velocities measured on horizontal surfaces vary from  
 222  $1.2 \cdot 10^{-5} \text{ m s}^{-1}$  on conventional glass for  $u_{ref} = 1.3 \text{ m s}^{-1}$ , to  $1.4 \cdot 10^{-3} \text{ m s}^{-1}$  on synthetic grass for  
 223  $u_{ref} = 9.9 \text{ m s}^{-1}$ . Thus there is a factor of over two orders of magnitude between the lowest and highest  
 224 values measured on these urban surfaces.

225 Table 2: average  $V_d$  as a function of  $u_{ref}$ .

u <sub>ref</sub> (m s <sup>-1</sup> )	V <sub>d</sub> (x 10 <sup>-5</sup> m s <sup>-1</sup> )				
	Glass		Cement facing		Synthetic grass
	Horizontal	Vertical	Horizontal	Vertical	
1.3	1.4 ± 0.4		2.2 ± 0.9	1.4 ± 0.3	28.1 ± 8.4
5.0	2.3 ± 1.3	1.1 ± 0.4	4.8 ± 1.8	3.6 ± 0.7	54.6 ± 19.3
9.9	4.5 ± 2.0	2.4 ± 0.3	7.2 ± 1.6	8.0 ± 2.0	124.7 ± 29.6

226  
 227 Those measured on vertical surfaces vary from  $1.1 \cdot 10^{-5} \text{ m s}^{-1}$  on conventional glass for  $u_{ref} = 5.0 \text{ m s}^{-1}$  to  
 228  $8.0 \cdot 10^{-5} \text{ m s}^{-1}$  on cement facing for  $u_{ref} = 9.9 \text{ m s}^{-1}$ . The dry deposition velocity  $V_d$  could not be measured  
 229 on vertical conventional glass for  $u_{ref} = 1.3 \text{ m s}^{-1}$  during the experimental campaign.

### III.2 Turbulent parameters

Aerodynamic parameters determined by hot wire measurements are listed in Table 3. All the developed boundary layers are turbulent at fetches of 1.1, 5.1 and 6.9 m, with a transition zone to the logarithmic profile (Fig. 4). The friction velocities are determined by fitting the logarithmic relation (5) to the mean velocity profiles. The estimated friction velocities decrease for an increasing fetch. This variation is consistent with the reduction in the stress at the wall  $\tau_p$  upon development of a completely turbulent boundary layer (Antonia and Luxton, 1971). The representation of the profiles in terms of dimensionless velocity  $(u + \Delta u)^+$  and dimensionless vertical position  $(z + d)^+$  ( $u^+ = u / u_*$ ;  $z^+ = z u_* / \nu$ , with  $\nu$  the kinematic viscosity of air) and the mean velocity shifts values  $\Delta u$ , with  $\Delta u = \ln z_0^+ + C$  ( $C = 5$ ), show the different rough regimes of the flows generated by each surface type at each  $u_{ref}$  (Krogstad and Antonia, 1999). The profiles of  $I_u$  and  $I_w$  were calculated using (7.a) and (7.b), and profiles of  $I_w$  are shown in Fig. 5. All the profiles over  $u$  and  $w$  have the same shape, with a maximum  $I_{wmax}$  in the immediate vicinity of the surface. The calculated values are shown in Table 3. For equal  $u_{ref}$ , the values of  $I_{umax}$  and  $I_{wmax}$  are higher for synthetic grass than for cement facing, and higher for cement facing than for glass, with  $I_{umax}$  greater than  $I_{wmax}$ . These observations are consistent with the observations of Antonia and Luxton (1971) for a boundary layer on a rough surface. Unlike the friction velocities, these relative turbulence intensities show no notable decrease as a function of the fetch but are essentially constant at each fetch for the same surface at the same flow speed.

### III.3 Discussions

The average deposition velocities for each type of surface and each  $u_{ref}$  (Table 2) have been compared to the data of the literature (Fig. 6). The deposition velocities measured in this study are of the same order of magnitude as those in the literature for smooth surfaces and grass. The absence of data on the geometry of the surface roughnesses studied by Toprak et al. (1997) makes it impossible to understand the differences in the measured  $V_d$ . The dry deposition velocities vary with the mean air flow speed, the surface type and the orientation of the surface. On horizontal surfaces,  $V_d$  varies on average by a factor of 1.7 and 23.7 respectively between conventional glass and cement facing and between conventional glass and synthetic grass, and by a factor of 1.9 and 3.6 between  $u_{ref} = 1.3 \text{ m s}^{-1}$  and  $u_{ref} = 5.0 \text{ m s}^{-1}$  and between  $u_{ref} = 1.3 \text{ m s}^{-1}$  and  $u_{ref} = 9.9 \text{ m s}^{-1}$  respectively.

Table 3: aerodynamic parameters for each surface as a function of  $u_{ref}$  and the fetch.

Fetch (m)	$u_{ref}$ (m s <sup>-1</sup> )	Conventional glass					Cement facing						Synthetic grass					
		$V_d$	$u_*$	$z_0$	$I_{umax}$	$I_{wmax}$	$V_d$	$u_*$	$z_0$	$d$	$I_{umax}$	$I_{wmax}$	$V_d$	$u_*$	$z_0$	$d$	$I_{umax}$	$I_{wmax}$
		(10 <sup>-4</sup> m s <sup>-1</sup> )	(m s <sup>-1</sup> )	(10 <sup>-2</sup> mm)	(%)	(%)	(10 <sup>-4</sup> m s <sup>-1</sup> )	(m s <sup>-1</sup> )	(10 <sup>-2</sup> mm)	(mm)	(%)	(%)	(10 <sup>-4</sup> m s <sup>-1</sup> )	(m s <sup>-1</sup> )	(mm)	(mm)	(%)	(%)
1.1		1.7					3.1						3.3	0.17	4.4	23.9	38.3	18.7
5.1	1.3	1.2	0.06	8.5	25.4	7.2	1.9	0.07	0.1	5.6	25.8	7.4	2.6	0.13	4.4	20.9	33.5	14.9
6.9		1.1	0.06	8.7	24.7	7.5	1.8	0.07	0.1	4.5	26.8	7.0	2.6	0.13	4.4	16.1	35.3	16.6
1.1		2.8	0.26	9.9	23.6	10.1	4.9	0.33	0.1	6.4	21.2	11.0	7.0	0.67	4.4	24.0	44.7	23.7
5.1	5.0	1.4	0.23	4.2	21.2	8.7	4.3	0.29	0.1	4.0	24.3	10.1	5.8	0.52	4.4	17.6	47.6	24.9
6.9		2.2	0.20	1.9	21.2	8.1	5.2	0.27	0.1	2.5	24.0	10.2	3.9	0.56	4.4	13.1	42.5	23.4
1.1		5.6	0.50	5.9	19.1	9.3	7.6	0.66	0.1	5.1	22.8	11.7	13.1	1.37	4.4	24.0	46.6	26.0
5.1	9.9	2.9	0.46	3.1	18.7	8.6	6.5	0.54	0.1	4.0	23.5	10.5	12.1	1.06	4.4	15.6	44.7	25.6
6.9		6.3	0.38	1.5	16.9	8.9	7.4	0.54	0.1	2.8	25.4	11.2	12.1	1.05	4.4	9.0	44.6	24.8

262

263 These results show the importance of turbulent processes of interception and impaction for this size  
 264 range of particles, dependent respectively on the sizes of the aerosol and the obstacle, and on the Stokes  
 265 number (itself dependent on the relaxation time of the aerosol, the flow speed and the size of the  
 266 obstacle). Moreover, the measured differences in deposition velocities between horizontal and vertical  
 267 walls, conventional glass and cement facing are on the order of the sedimentation velocity for the  
 268 fluorescein aerosol calculated with (7) from the distribution of Fig 2.

$$V_s = \sum_{i=1}^{12} \frac{d_{pi}^2 g C_{ui} \rho}{18\nu} m_{ni} = 1.10 \pm 0.37 \cdot 10^{-5} \text{ m s}^{-1} \quad (7)$$

269 Here,  $g$  is the gravitational acceleration ( $9.81 \text{ m s}^{-2}$ ),  $\rho$  is the density of the particles ( $1000 \text{ kg m}^{-3}$  for  
 270 aerodynamic diameters determined with a cascade impactor,)  $C_{ui}$  is the Cunningham correctional factor  
 271 for the aerosol of diameter  $d_{pi}$  (geometric diameter of stage  $i$  of the cascade impactor),  $\nu$  is the kinematic  
 272 viscosity of air ( $1.5 \cdot 10^{-5} \text{ m}^2 \text{ s}^{-1}$ ) and  $m_{ni}$  is the fluorescein mass on stage  $i$  normalised to the total mass of  
 273 fluorescein collected on the 12 stages. For low wind speeds, the contribution of sedimentation to  
 274 deposition of this fluorescein aerosol is therefore non-negligible, contrary to what is usually believed for  
 275 submicron aerosols. It can double the deposition velocity between a vertical wall and a horizontal wall, or  
 276 even represent the entire deposit on a smooth horizontal wall for a low wind speed, as for glass with  
 277  $u_{ref} = 1.3 \text{ m s}^{-1}$ . It should also be noted that deposition velocities on horizontal and vertical cement facing  
 278 are approximately equal at  $u_{ref} = 9.9 \text{ m s}^{-1}$ . As the deposition flux depends on the vertical wind speed and  
 279 its fluctuations, the deposition velocity  $V_d$  is shown in Fig. 7 as a function of the maximum relative  
 280 turbulence intensity over  $w$ ,  $I_{wmax}$ . An increase in deposition flux with turbulence intensity was already  
 281 observed by Dai *et al.* (2001) for a smooth surface. Our graph shows a variation in  $V_d$  as a function of  $I_{wmax}$   
 282 independent of a particular type of surface. This observation is of interest as it represents  $V_d$  as a function  
 283 of a single turbulent parameter for several surface types.

284 The parameter usually related to  $V_d$  is the friction velocity  $u_*$ , as it quantifies the turbulence in a boundary  
 285 layer. It is one of the main parameters used in the deposition models developed for inside and outside  
 286 environments. The calculated deposition velocities for the polydispersed fluorescein aerosol with the  
 287 models of Lai and Nazaroff (2000) and of Zhang *et al.* (2001) (with zero aerodynamic resistance, because  
 288 the concentration above the surface is consistent with that measured in the centre of the test section),  
 289 and the data of this study are shown as a function of  $u_*$  in Fig. 8. The friction velocities of the vertical  
 290 surfaces associated with the  $V_d$  are those estimated for the same horizontal surfaces and same  $u_{ref}$  at the



fetch 5.0 m. The model of Lai and Nazaroff (2000) correctly estimates the deposition velocities on glass for  $u_*$  greater than  $0.2 \text{ m s}^{-1}$ , but seems to overestimate them below this for horizontal glass.

On the other hand, Zhang *et al.* (2001) systematically overestimate  $V_d$  on grass by more than a factor of 5. This resistive model uses Brownian diffusion as the principal deposition process for a submicron aerosol deposition on grass and underestimates interception and impaction processes. By comparison, the recent mechanistic model of Petroff *et al.* (2008) accords more importance to interception for this aerosol size range. It is in a better agreement with Chamberlain (1967) data on grass in a wind tunnel for micron and submicron aerosols than Zhang *et al.* (2001). This shows the limits of the operational model of Zhang *et al.* (2001) in assessing  $V_d$  on grass precisely, and the need to either improve consideration of turbulent processes in deposition on grass, or to estimate  $V_d$  from mechanistic models like that of Petroff *et al.* (2008) that better account for these turbulent processes.

In the literature, dry deposition velocities measured *in situ* are generally normalised to  $u_*$ . In this case, the sedimentation velocity  $V_s$  (7), a non-turbulent deposition process, must be subtracted from  $V_d$ . In recent studies of transfers in natural environments, the ratio of  $V_d$  and  $u_*$  was found to be independent of the various surfaces studied under neutral and stable conditions and approximately equal to  $2 \cdot 10^{-3}$  (Damay, 2010; Donateo *et al.*, 2010). On the contrary, in this study, this ratio depends on the type of surface (Fig. 9) and thus on the flow conditions and the structure of the boundary layer. It is therefore determined by the importance of interception and impaction in the deposition process. The ratio is  $5.3 \pm 4.1 \cdot 10^{-5}$  for conventional glass,  $1.5 \pm 0.6 \cdot 10^{-4}$  for cement facing, and  $1.3 \pm 0.3 \cdot 10^{-3}$  for synthetic grass. The experimental results are close to the estimate of the model of Lai and Nazaroff (2000) for glass ( $5.0 \pm 0.1 \cdot 10^{-5}$ ) and the *in situ* values of Damay (2010) on a grassland,  $0.8 \cdot 10^{-3}$  and  $1.6 \cdot 10^{-3}$  respectively for  $d_p = 0.20$  and  $0.32 \text{ }\mu\text{m}$ , for synthetic grass.

In the urban canopy, in the urban sub-layer of the atmospheric boundary layer, measurable friction velocity  $u_*$  in the boundary layers of the surfaces is not obvious. Use of  $u_*$  alone as a turbulent parameter seems thus to be limited in modelling deposition on heterogeneous urban surfaces. As an initial approach, in the context of operational models to give quick estimates of deposition velocities, wind speed in the streets could turn out to be a good parameter, as it is easily measurable or modelled. Empirical parameterisation of  $V_d$  as a linear function of  $u_{\text{ref}}$  for each type of surface according to the data of Table 2 could be a good first approximation.

## 320 IV. Conclusions

321 Presently, there is little experimental data on dry deposition velocities for the urban environment. This  
322 wind tunnel study was conducted to measure  $V_d$  and the associated turbulent parameters for a  
323 polydispersed submicron aerosol on urban surfaces. The deposition velocity  $V_d$  was measured on three  
324 urban surfaces types, horizontal and vertical, and for three flow speeds  $u_{ref}$ , and these data were  
325 compared to the data of other authors. These deposition velocities show dependence on both  $u_{ref}$  and the  
326 type of deposition surface, confirming the importance of the turbulent processes of interception and  
327 impaction in deposition for an aerosol of this size. However, sedimentation is responsible for a large part  
328 of the deposition for smooth horizontal surfaces and for low  $u_{ref}$ . The model of Lai and Nazaroff (2000)  
329 correctly estimates  $V_d$  on glass, while Zhang *et al.* (2001) substantially overestimate it on grass. Finally,  
330 this work reveals that parameterisation of  $V_d$  as a function of  $u_{ref}$  may be relevant for the urban  
331 environment in an operational context.

332 This wind tunnel study treats only a limited number of parameters and types of surfaces. However, it  
333 highlights the absence of a single parameterisation for the deposition velocity as a function of  
334 aerodynamic parameters for smooth or rough surfaces. This absence is certainly due to the lack of  
335 reported data with turbulent parameters and the lack of deposition experiments on rough walls, even for  
336 simple roughness geometries. In the case of pollution by radionuclides, the disparity in the deposition  
337 velocities about two orders of magnitude measured in this study shows the importance of a local estimate  
338 of depositions in the urban canopy for each surface, rather than an estimate on the scale of entire  
339 neighbourhoods. Finally, a wind tunnel study can only constitute a first step in studying dry deposition in  
340 the urban environment and should be supplemented by *in situ* measurements.

## 341 V. REFERENCES

- 342 Antonia R. A., Luxton R. E., 1971. The response of a turbulent boundary layer to a step change in surface  
343 roughness, part 1. Smooth to rough. Journal of Fluid Mechanics 48, 721-761.
- 344 Chamberlain A.C., 1967. Transport of Lycopodium spores and other small particles to rough surfaces.  
345 Proceedings of the Royal Society London, 296 A.
- 346 Dai W., Davidson C.I., Etyemezian V., Zufall M., 2001. Wind tunnel studies of particles transport and  
347 deposition in turbulent boundary flows. Aerosol Science and Technology 35, 887-898.

348 Damay P., 2010. Détermination expérimentale de la vitesse de dépôt sec des aérosols submicroniques  
 349 en milieu naturel: influence de la granulométrie, des paramètres micrométéorologiques et du couvert.  
 350 Thèse de doctorat de l'INSA de Rouen.

351 Donato A., Damay P. E., Contini D., Maro D., Roupsard P., 2010. Similarities and differences in dry  
 352 deposition velocity normalized to friction velocity over maize, grass, bare soil and ice measured with  
 353 different instruments. International Aerosol Conference 2010, Helsinki.

354 Flori J.P., Giraud D., Olive F., Ruot B., Sini J.F, Rosant J.M., Mestayer P., Connan O., Maro D., Hébert  
 355 D., Rozet M., Talbaut M., Coppalle A., 2007. Salissures de façades (SALIFA), Programme PRIMEQUAL,  
 356 rapport final. EN-CAPE 07.129 C.

357 Fowler D., Pilegaard K., Sutton M.A., Ambus P., Raivonen M., Duyzer J., Simpson D., Fagerli H., Fuzzi  
 358 S., Schjoerring J.K., Granier C., Neftel A., Isaksen I.S.A., Laj P., Maione M., Monks P.S., Bukhardt J.,  
 359 Daemmgen U., Neiryneck J., Personne E., Wichink-Kruit R., Butterbach-Bahl K., Flechard C., Tuovinen  
 360 J.P., Coyle M., Gerosa G., Loubet B., Altimir N., Gruenhage L., Ammann C., Cieslik S., Paoletti E.,  
 361 Mikkelsen T.N., Ro-Poulsen H., Cellier P., Cape J.N., Horváth L., Loreto F., Niinemets U., Palmer P.I.,  
 362 Rinne J., Misztal P., Nemitz E., Nilsson D., Pryor S., Gallagher M.W., Vesala T., Skiba U., Brüggemann  
 363 N., Zechmeister-Boltenstern S., Williams J., O'Dowd C., Facchini M.C., de Leeuw G., Flossman A.,  
 364 Chaumerliac N., Erisman J.W., 2009. Atmospheric composition change: Ecosystems-Atmosphere  
 365 interactions. Atmospheric Environment 43, 5193-5267.

366 Gründel M., Porstendörfer J., 2004. Differences between the activity size distributions of the different  
 367 natural radionuclide aerosols in outdoor air. Atmospheric Environment 38, 3723-3728.

368 Horvath H., Pesava P., Toprak S., Aksu R., 1996. Technique for measuring the deposition velocity of  
 369 particulate matter to building surfaces. The Science of the Total Environment 189/190, 255-258.

370 Jaenicke R., 1988. Aerosol physics and chemistry. In Landolt-Börstein. Numerical data and functional  
 371 relationships in science and technology, Group V, Vol. 4 Meteorology, subvolume b Physical and  
 372 chemical properties of the air. Springer-Verlag, Berlin.

373 Kelly G.N., 1987. The importance of the urban environments for accident consequences. Radiation  
 374 Protection Dosimetry 21, 13-20.

375 Krogstad P.Å., Antonia R.A., 1999. Surface roughness effects in turbulent boundary layers. Experiments  
376 in fluids 27, 450-460.

377 Lai A.C.K., Nazaroff W.W., 2000. Modeling indoor particle deposition from turbulent flow onto smooth  
378 surfaces. Journal of Aerosol Science 31, 463-476.

379 Liu B. Y. H., Agarwal J. K., 1974. Experimental observation of aerosol deposition in turbulent flow.  
380 Aerosol Science 5, 145-155.

381 Maro, D., Connan, O., Hébert, D., Rozet, M., Talbaut, M., Coppalle, A., Sini, J.F., Rosant, J.M., Mestayer,  
382 P., Sacré, C., Flori, J.P., Giraud, D., Olive, F., Ruot, B., Roupsard, P., 2010. Quantification of the dry  
383 deposition of aerosols in an urban environment: towards a new methodology. International Aerosol  
384 Conference 2010, Helsinki.

385 NF X 44-011, 1972. Séparateurs aérauliques. Méthode de mesure de l'efficacité des filtres au moyen  
386 d'un aérosol d'uranine (fluorescéine). AFNOR, La Plaine Saint-Denis.

387 Papastefanou C., 2006. Residence time of tropospheric aerosols in association with radioactive nuclides.  
388 Applied Radiations and Isotopes 64, 93-100.

389 Papastefanou C., 2008. Radioactivity in the Environment, Volume 12, Chapter 1, Atmospheric Aerosol  
390 Particles. Elsevier Science, Oxford.

391 Pesava P., Aksu R., Toprak S., Horvath H., Seidl S., 1999. Dry deposition of particles to building surfaces  
392 and soiling. The Science of the Total Environment 235, 25-35.

393 Petroff A., Mailliat A., Amielh M, Anselmet F., 2008. Aerosol dry deposition on vegetative canopies. Part  
394 II: a new modelling approach and applications. Atmospheric Environment 42, 3654-3683.

395 Raupach M. R., Antonia R. A., Rajagopalan S., 1991. Rough-wall turbulent boundary layers. Applied  
396 Mechanics Reviews 44, 1-25.

397 Roed J., 1983. Deposition velocity of caesium-137 on vertical building surfaces. Short Communication,  
398 Atmospheric Environment 17, 663-664.

399 Roed J., 1985. Dry deposition of urban surfaces. Risø-R-515 NKA/REK-1(84)701, Risø National  
400 Laboratory, Roskilde.

401 Roed J., 1987. Dry deposition in rural and in urban areas in Denmark. *Radiation Protection Dosimetry* 21,  
402 33-36.

403 Schlichting H., 1968. *Boundary-Layer Theory*. McGraw Hill, New York.

404 Sehmel G.A., 1980. Particle and gas dry deposition: a Review. *Atmospheric Environment* 14, 983-1011.

405 Toprak S., Aksu R., Pesava P., Horvath H., 1997. The soiling of materials under simulated atmospheric  
406 conditions in a wind tunnel. *Journal of Aerosol Science* 28, Supplement 1, S585-S586.

407 Van Dingenen R., Raes F., Putaud J.P., Baltensperger U., Charron A., Facchini M.-C., Decesari S., Fuzzi  
408 S., Gehrig R., Hansson H.-C., Harrison R.M., Hüglin C., Jones A.M., Laj P., Lorbeer G., Maenhaut W.,  
409 Palmgren F., Querol X., Rodriguez S., Schneider J., ten Brink H., Tunved P., Tørseth K., Wehner B.,  
410 Weingartner E., Wiedensohler A., Wählin P., 2004. A European aerosol phenomenology – 1: physical  
411 characteristics of particulate matter at kerbside, urban, rural and background sites in Europe.  
412 *Atmospheric Environment* 38, 2561-2577.

413 Zhang L., Gong S., Padro J., Barrie L., 2001. A size-segregated particle dry deposition scheme for an  
414 atmospheric aerosol module. *Atmospheric Environment* 35, 549-560.

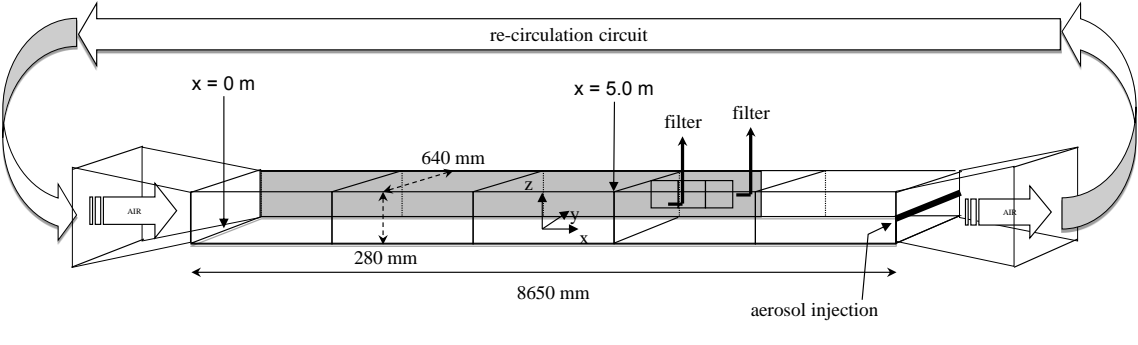
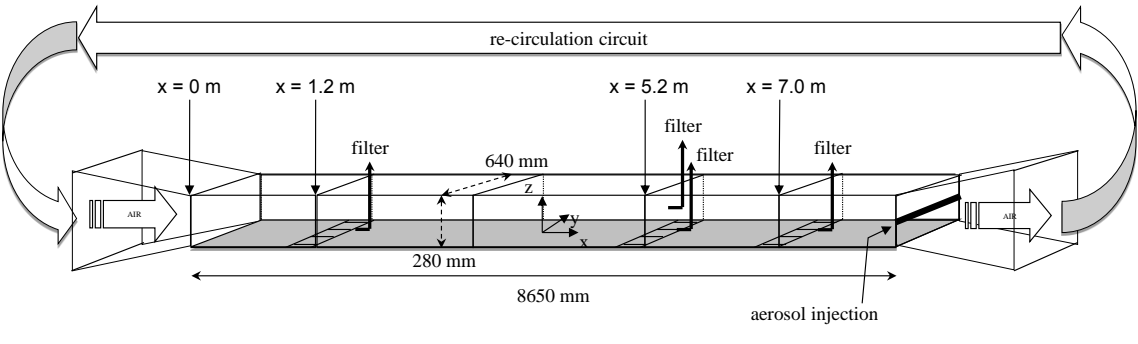


Fig. 1: illustrations of the wind tunnel configurations to study deposition on horizontal (a) and vertical (b) walls; the studied surface is grey; the substrates samples are the grey squares.

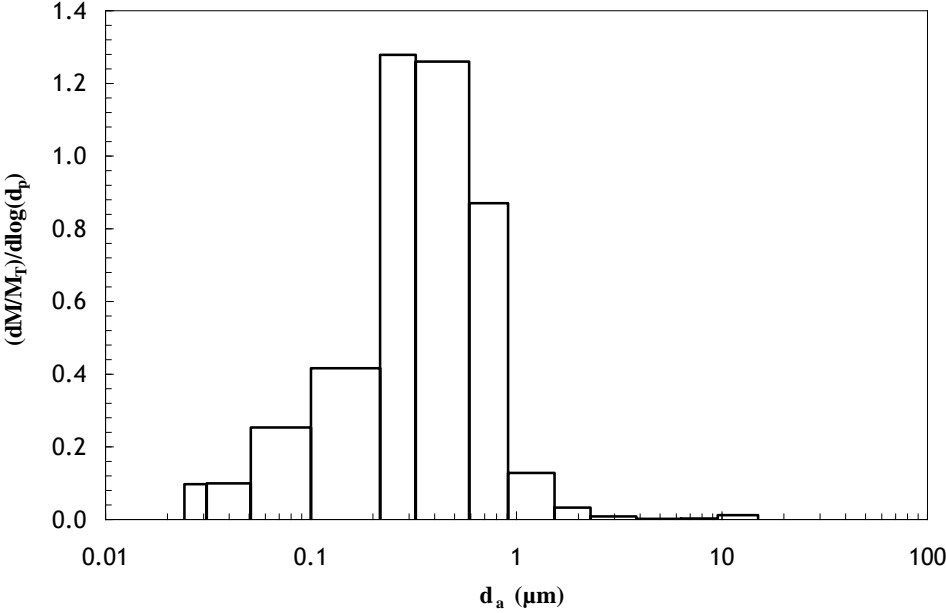


Fig. 2: normalised granulometric mass distribution of the fluorescein aerosol.

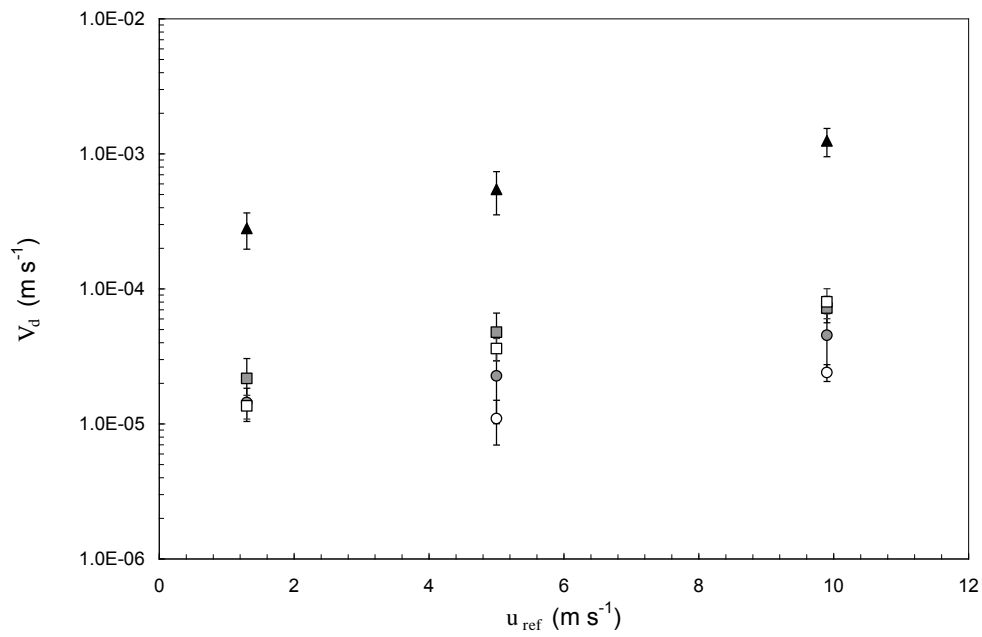
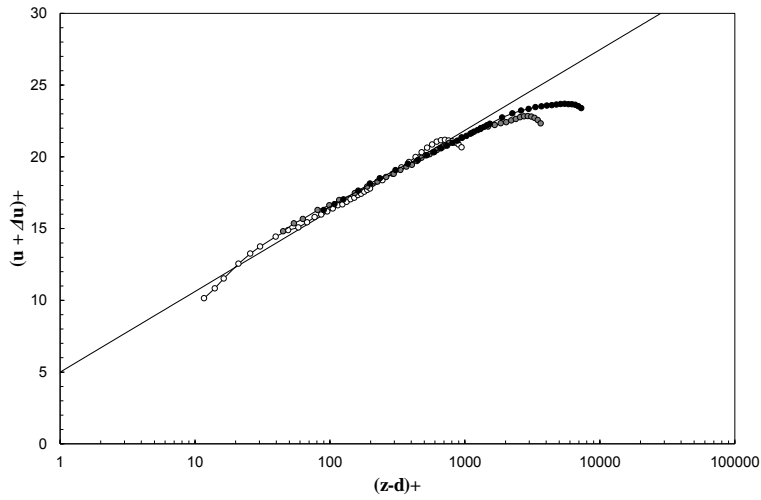


Fig. 3: average  $V_d$  as a function of  $u_{ref}$ .

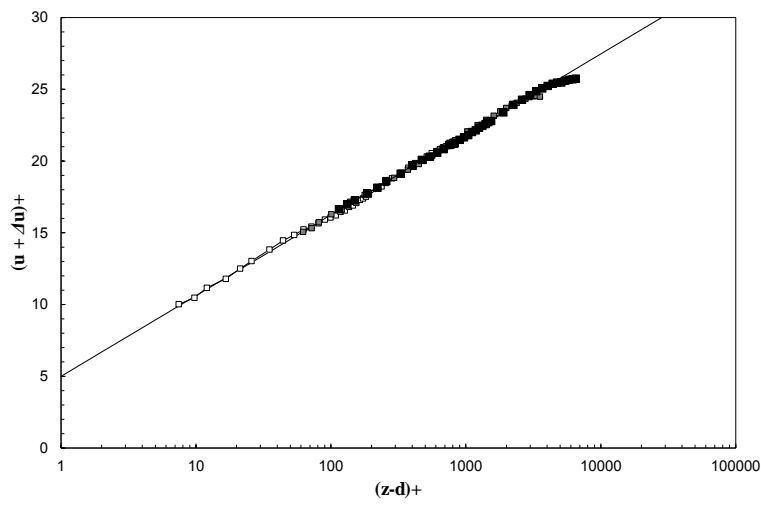
● Horizontal conventional glass; ○ Vertical conventional glass;

■ Horizontal cement facing; □ Vertical cement facing;

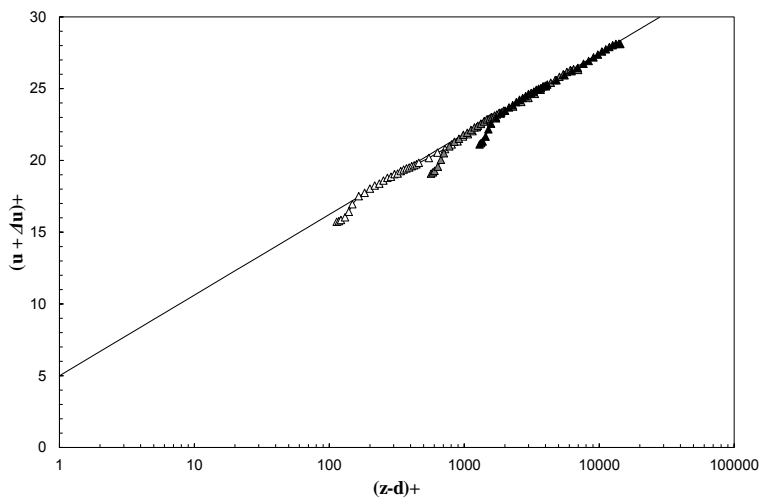
▲ Synthetic grass.



26 a)



27 b)



28 c)

29 Fig. 4:  $u_+$  as a function of  $z_+$  for a fetch of 5.10 m for each type of surface and each  $u_{ref}$ .

30 a) Conventional glass:  $\circ$   $u_{ref} = 1.3 \text{ m s}^{-1}$ ;  $\bullet$   $u_{ref} = 5.0 \text{ m s}^{-1}$ ;  $\bullet$   $u_{ref} = 9.9 \text{ m s}^{-1}$ ;

31 b) Cement facing:  $\square$   $u_{ref} = 1.3 \text{ m s}^{-1}$ ;  $\blacksquare$   $u_{ref} = 5.0 \text{ m s}^{-1}$ ;  $\blacksquare$   $u_{ref} = 9.9 \text{ m s}^{-1}$ ;

32 c) Synthetic grass:  $\triangle$   $u_{ref} = 1.3 \text{ m s}^{-1}$ ;  $\triangle$   $u_{ref} = 5.0 \text{ m s}^{-1}$ ;  $\blacktriangle$   $u_{ref} = 9.9 \text{ m s}^{-1}$ .

33



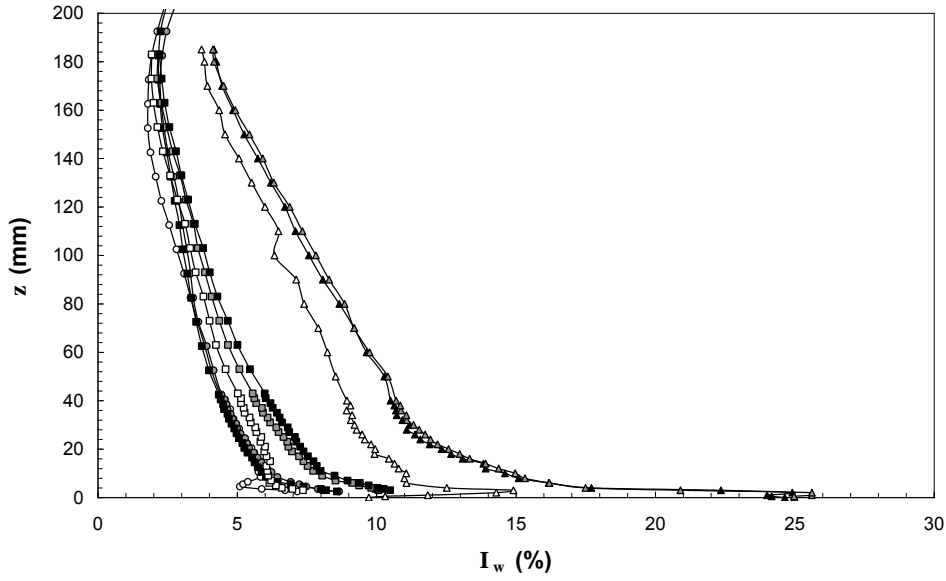


Fig. 5:  $I_w$  as a function of  $z$  for a fetch of 5.10 m, for each surface type and each  $u_{ref}$ .

Conventional glass:  $\circ$   $u_{ref} = 1.3 \text{ m s}^{-1}$ ;  $\bullet$   $u_{ref} = 5.0 \text{ m s}^{-1}$ ;  $\bullet$   $u_{ref} = 9.9 \text{ m s}^{-1}$ ;

Cement facing:  $\square$   $u_{ref} = 1.3 \text{ m s}^{-1}$ ;  $\blacksquare$   $u_{ref} = 5.0 \text{ m s}^{-1}$ ;  $\blacksquare$   $u_{ref} = 9.9 \text{ m s}^{-1}$ ;

Synthetic grass:  $\triangle$   $u_{ref} = 1.3 \text{ m s}^{-1}$ ;  $\triangle$   $u_{ref} = 5.0 \text{ m s}^{-1}$ ;  $\blacktriangle$   $u_{ref} = 9.9 \text{ m s}^{-1}$ .

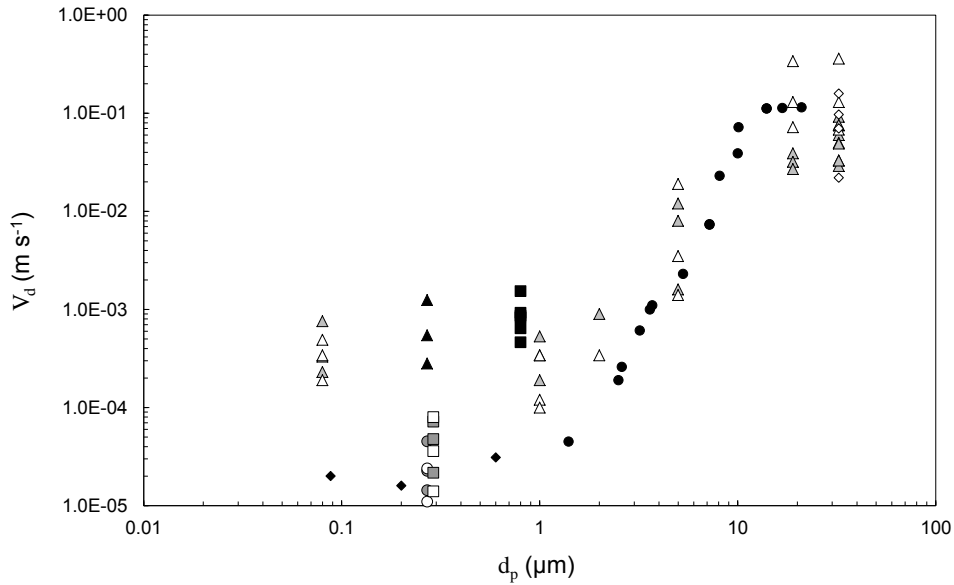


Fig. 6: mean  $V_d$  of this study and  $V_d$  from the literature as a function of  $d_p$ .

● Vertical glass (Liu and Agarwal, 1974); ◆ Glass (Horvath *et al.*, 1996); ◇ horizontal sticky rough glass (Chamberlain, 1967); ■ Cement (Toprak *et al.*, 1997); △ Sticky artificial grass, ▲ Real grass (Chamberlain, 1967);

This study: ● Horizontal conventional glass; ○ Vertical conventional glass;

■ Horizontal cement facing; □ Vertical cement facing;

▲ Synthetic grass.

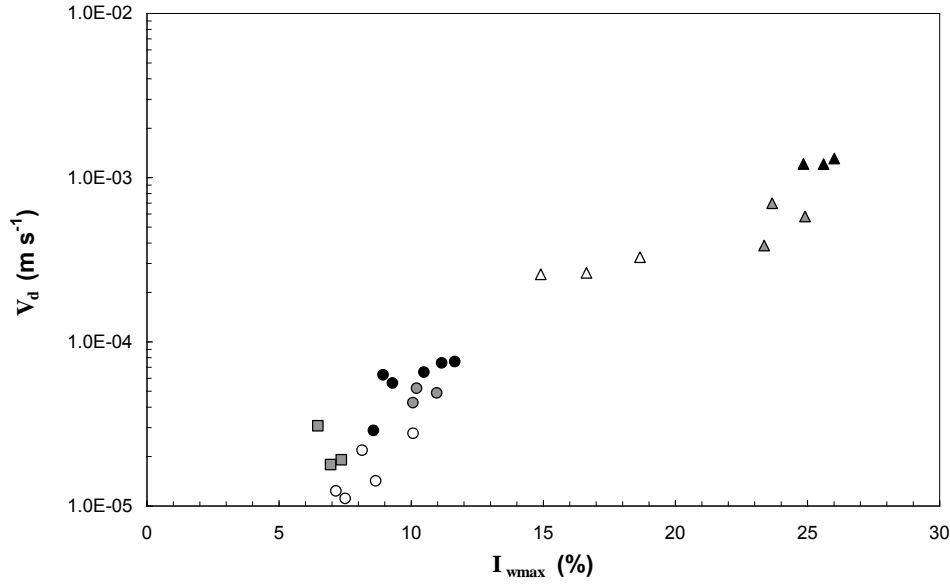


Fig. 7: average  $V_d$  as a function of  $I_{wmax}$  for each type of surface.

Conventional glass:  $\circ$   $u_{ref} = 1.3 \text{ m s}^{-1}$ ;  $\bullet$   $u_{ref} = 5.0 \text{ m s}^{-1}$ ;  $\bullet$   $u_{ref} = 9.9 \text{ m s}^{-1}$ ;

Cement facing:  $\square$   $u_{ref} = 1.3 \text{ m s}^{-1}$ ;  $\blacksquare$   $u_{ref} = 5.0 \text{ m s}^{-1}$ ;  $\blacksquare$   $u_{ref} = 9.9 \text{ m s}^{-1}$ ;

Synthetic grass:  $\triangle$   $u_{ref} = 1.3 \text{ m s}^{-1}$ ;  $\triangle$   $u_{ref} = 5.0 \text{ m s}^{-1}$ ;  $\blacktriangle$   $u_{ref} = 9.9 \text{ m s}^{-1}$ .

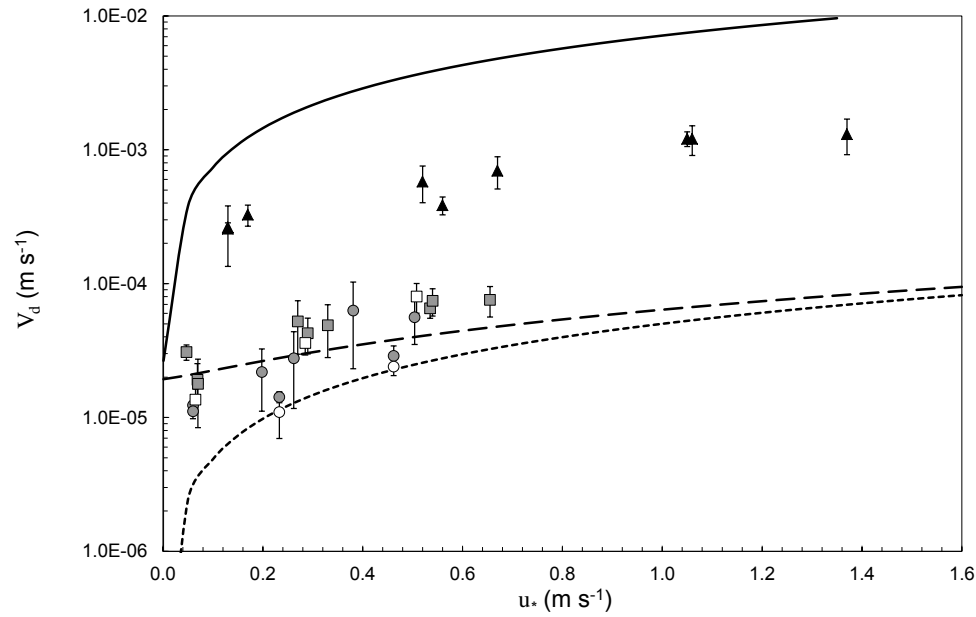


Fig. 8:  $V_d$  as a function of  $u_*$ , comparison of model to measurements.

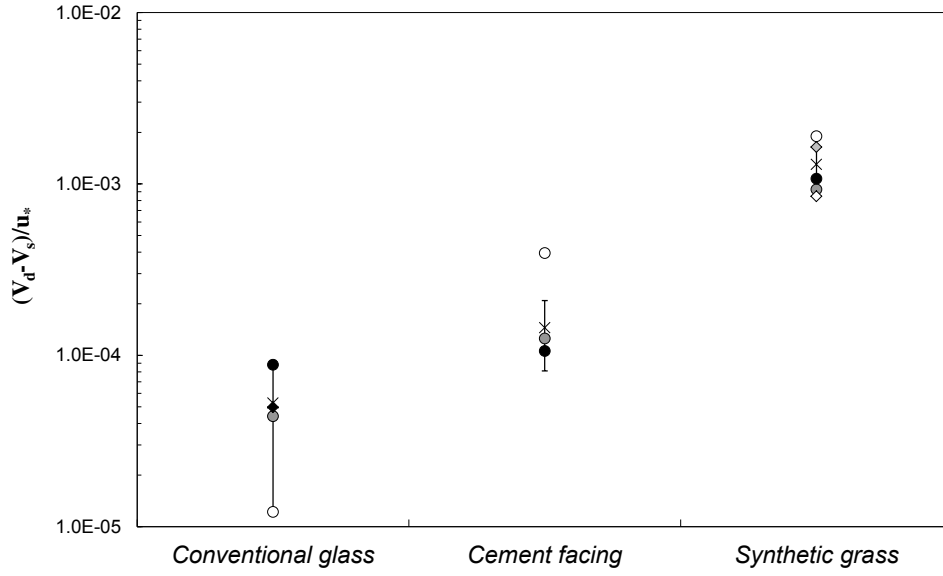
--- Horizontal smooth wall, - - - Vertical smooth wall (Lai and Nazaroff, 2000);

— Grass (Zhang *et al.*, 2001);

This study:  $\bullet$  Horizontal conventional glass;  $\circ$  Vertical conventional glass;

$\blacksquare$  Horizontal cement facing;  $\square$  Vertical cement facing;

$\blacktriangle$  Synthetic grass.



59

60 Fig. 9:  $\frac{V_d - V_s}{u_*}$  ratios for each type of horizontal surface.

61 ♦ Smooth wall (Lai and Nazaroff, 2000);

62 ◇ Grass ( $d_p = 0.202 \text{ } \mu\text{m}$ ), ◇ Grass ( $d_p = 0.316 \text{ } \mu\text{m}$ ) (Damay, 2010);

63 This study: ○  $u_{ref} = 1.3 \text{ m s}^{-1}$ ; ●  $u_{ref} = 5.0 \text{ m s}^{-1}$ ; ●  $u_{ref} = 9.9 \text{ m s}^{-1}$ ; x mean on all  $u_{ref}$  for each surface.